

## Feasibility of photovoltaic – Thermoelectric hybrid modules

W.G.J.H.M. van Sark\*

Dept. Science, Technology and Society, Copernicus Institute, Utrecht University, Budapestlaan 6, 3584 CD Utrecht, The Netherlands

### ARTICLE INFO

#### Article history:

Received 15 November 2010  
Received in revised form 4 February 2011  
Accepted 8 February 2011  
Available online 4 March 2011

#### Keywords:

Thermoelectric conversion  
Photovoltaic solar energy  
Solar cells  
Modelling

### ABSTRACT

Outdoor performance of photovoltaic (PV) modules suffers from elevated temperatures. Conversion efficiency losses of up to about 25% can result, depending on the type of integration of the modules in the roof. Cooling of modules would therefore enhance annual PV performance. Instead of module cooling we propose to use the thermal waste by attaching thermoelectric (TE) converters to the back of PV modules, to form a PV–TE hybrid module. Due to the temperature difference over the TE converter additional electricity can be generated. Employing present day thermoelectric materials with typical figure of merits ( $Z$ ) of  $0.004 \text{ K}^{-1}$  at 300 K may lead to efficiency enhancements of up to 23% for roof integrated PV–TE modules, as is calculated by means of an idealized model. The annual energy yield would increase by 14.7–11%, for two annual irradiance and temperature profiles studied, i.e., for Malaga, Spain, and Utrecht, the Netherlands, respectively. As new TE materials are being developed, efficiency enhancements of up to 50% and annual energy yield increases of up to 24.9% may be achievable. The developed idealized model, however, is judged to overestimate the results by about 10% for practical PV–TE hybrids.

© 2011 Elsevier Ltd. All rights reserved.

### 1. Introduction

Outdoor performance of photovoltaic (PV) modules or panels suffers from the high temperatures reached under high irradiation conditions in combination with the negative temperature coefficient of efficiency. Depending on integration type temperatures of panels can reach 60–80 °C, resulting in a loss in efficiency of about 20%, see, e.g., Drews [1]. Cooling of the PV panels would enhance their (annual) performance. However, active cooling systems based on either air or water do not only need electric power to operate the cooling system but also waste the transferred heat into the environment. The latter is also the case for passive cooling systems that do not require electric power as input. In contrast to such systems, thermoelectric (Peltier) cooling elements attached to the back of a PV panel could make use of the either heated air or water. This is particularly interesting for concentrated PV concepts. Cooling of PV cells under concentrated sunlight has been reviewed by Royne et al. [2].

It has been reported that the heat produced in the PV panel can be used for heating of water, thereby cooling the PV panel. Such a micro combined heat and power ( $\mu$ CHP) [3] unit usually is denoted as a PVT (PV–Thermal) panel [4,5], and the total efficiency of a PVT panel is larger than the sum of the efficiencies of a separate PV panel and a solar thermal collector on a per unit area basis. The temperature difference with ambient temperature can be used to generate additional power using the thermoelectric (TE) effect, so

to reach a larger overall efficiency of a so-called PV–TE hybrid system [6–10]. In this way, waste heat is extracted by cooling, but as the cooling medium may rise in temperature, the conversion efficiency may be limited [11]. Other applications for TE power generation are numerous, see, e.g., [12,13]. The amount of additional TE power is determined by the so-called figure of merit ( $Z$ ) of the TE material and the temperature difference over the TE module. The figure of merit  $Z$  depends on material parameters, i.e., Seebeck coefficient  $\alpha$  [V/K], thermal conductivity  $\lambda$  [W/cm K], and electrical resistivity  $\rho$  [ $\Omega$  cm], and is defined as  $Z = \alpha^2 \kappa / \rho$  [ $\text{K}^{-1}$ ] [14]. Usually the product of the figure of merit and temperature is quoted for a particular material, and present day materials have values of  $ZT \sim 1$  [9]. To increase the figure of merit, a good TE material, both  $n$ - and  $p$ -type doped material, is required to have a large Seebeck coefficient, high thermal conductivity, and low electrical resistivity [15].

Various thermoelectric materials exist, and based on the figure of merit value at a certain temperature are used in a number of applications with a specific temperature range. For example, the material lead telluride (PbTe) is used at temperatures between 600 and 800 K. At higher temperatures (800–1300 K) silicon germanium ( $\text{Si}_{1-x}\text{Ge}_x$ ) alloys are used, while at lower temperatures (200–400 K) bismuth telluride ( $\text{Bi}_2\text{Te}_3$ ) is preferred [9,14,16]. For all these materials and temperature ranges it holds that  $ZT$  is around 1. Recently, for a  $\text{Bi}_x\text{Sb}_{2-x}\text{Te}_3$  nanocrystal bulk alloy a  $ZT$  value of 1.2 at room temperature is reported ( $ZT = 1.4$  at 373 K) [17]. A  $p$ -type  $\text{BiSbTe/wt.}\% \text{ ZnAlO}$  composites has been prepared by zone melting method. The addition of 0.75 wt.% ZnAlO nanopowder into a  $(\text{Bi,Sb})_2\text{Te}_3$  matrix has lead to  $ZT \sim 1.1$  at 300 K

\* Tel.: +31 302537611; fax: +31 302537601.

E-mail address: [w.g.j.h.m.vansark@uu.nl](mailto:w.g.j.h.m.vansark@uu.nl)

[18]. New developments have lead to higher values of  $ZT \sim 1.5\text{--}4$  for various types of low-dimensional thermoelectric materials [19,20] such as (quantum dot) superlattices, as reviewed in [21], where a range of  $ZT \sim 1.5\text{--}2.5$  is reported for a temperature of 300 K. Nanostructured thermoelectric materials using colloidal inorganic nanocrystals ((Bi,Sb)<sub>2</sub>Te<sub>3</sub>) have recently been developed and show  $ZT = 0.7$  at room temperature [22]. Organic-based nanocomposites of PEDOT:PSS passivated Te nanorods show  $ZT = 0.1$ , using a water-based process [23]. Silicon nanowires of 20–300 nm in diameter have recently been reported to have  $ZT \sim 0.6$  at 300 K [24] and  $ZT \sim 1$  at 200 K [25]. With a further reduction of diameter, it is expected that  $ZT$  can be larger than 1 at 300 K [24], which would make silicon as a cheap and abundant material an excellent candidate for future TE devices [26].

The emergence of new high  $ZT$  materials warrants a study into the possible use of these materials in PV–TE hybrid systems. These systems have up to now hardly been studied because of the low conversion efficiency enhancements gained as a result of low  $ZT$  values. In this paper we demonstrate the performance enhancement resulting from attaching TE materials to the back of PV modules, thus creating a PV–TE hybrid system. We will first describe the system layout, followed by a description of a simple, idealistic model for the calculation of efficiency enhancement. This model includes the effect of irradiance and temperature on the performance of PV modules, as well as the effect of the figure of merit for the TE material. Then, using irradiation and temperature data for the Netherlands (city of Utrecht) and Spain (city of Malaga), on an hourly basis, annual performance of the PV–TE hybrid can be determined. Finally, future annual performance will be derived using realistically achievable figure of merit values of near-future TE materials.

## 2. System layout

A schematic overview of the system layout is depicted in Fig. 1. To the back side of the PV module a series of thermoelectric converters is attached. The heat generated in the PV module is converted to electricity by the series of thermoelectric converters, which are mounted on a heat sink. At high irradiance and high ambient temperatures, and depending on the type of integration, the module temperature can reach 80 °C. The temperature difference thus maximally is about 50–60 °C, therefore low-temperature TE materials are to be deployed, i.e. with  $ZT \geq 1$  at 300 K.

## 3. Model

### 3.1. Assumptions

Incident solar irradiation is converted by the PV module with efficiency  $\eta_{PV}$ . The remaining heat flux is assumed to be available to the TE module, and is converted with efficiency  $\eta_{TE}$ . Thus, the

heat flux through the module sides and front cover but especially radiation loss through the front cover are not taken into account. The total amount of generated power then is

$$P_{PVTE} = P_{PV} + P_{TE} = \eta_{PV}G + (1 - \eta_{PV})G\eta_{TE} \quad (1)$$

and the efficiency of the hybrid PVTE system is written as

$$\eta_{PVTE} = \eta_{PV} + (1 - \eta_{PV})\eta_{TE} \quad (2)$$

In the following we will show that all efficiencies depend on irradiance  $G$ .

### 3.2. PV simulation model

The PV module performance is modelled assuming constant maximum power point (MPP) operation. A simple parametric model for the efficiency  $\eta_{MPP}(G, T_M)$  as a function of irradiance  $G$  and module temperature  $T_M$  is used, see [1]. The effect of temperature on efficiency is modelled using a linear temperature dependence, with temperature coefficient  $\alpha$ :

$$\eta_{MPP}(G, T_M) = \eta_{MPP}(G, 25) \cdot (1 + \alpha(T_M - 25)) \quad (3)$$

and the efficiency  $\eta_{MPP}(G, T_M)$  at  $T_M = 25$  °C (standard test condition, STC) is given as

$$\eta_{MPP}(G, 25) = a_1 + a_2G + a_3 \ln(G) \quad (4)$$

with  $a_1, a_2, a_3$  module specific parameters.

The four parameters can in principle be determined from data sheets provided by manufacturers of PV modules, or from fitting measured efficiency data as a function of irradiance. In this paper we use constants derived from measurements of a multi-crystalline silicon module:  $a_1 = 0.1894$ ,  $a_2 = -0.04163 \text{ m}^2/\text{W}$ ,  $a_3 = 0.02158$ ,  $\alpha = -0.4\%/K$  [27].

In order to apply this model, the module temperature needs to be determined from the ambient temperature and irradiance, using the simplifying assumption that module temperature  $T_M$  to ambient temperature  $T_A$  difference is proportional to irradiance  $G$  [1]:

$$T_M = T_A + cG \quad (5)$$

The coefficient  $c$  is found to depend on the installation conditions, as shown in Table 1 (data from Sauer [28]).

### 3.3. TE simulation model

The efficiency of a TE module can be expressed as [14]:

$$\eta_{TE} = \eta_{Carnot} \frac{\sqrt{1 + T_{avg}Z} - 1}{\sqrt{1 + T_{avg}Z} + \frac{T_A}{T_M}} \quad (6)$$

with the Carnot efficiency defined as

$$\eta_{Carnot} = 1 - \frac{T_A}{T_M} \quad (7)$$

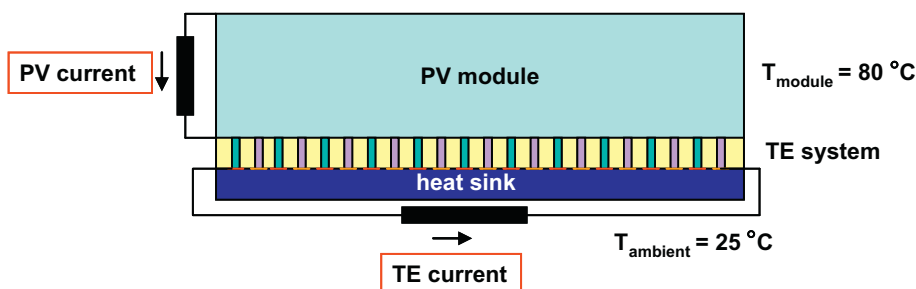


Fig. 1. Schematic overview of the PV–TE hybrid system with multiple thermoelectric generators consisting of n- and p-type doped semiconductor legs. At high irradiance and integration of the module in the roof the module temperature can reach 80 °C.

**Table 1**

Parameter  $c$  and module temperature  $T_M$  at  $G = 1000 \text{ W/m}^2$  and  $T_A = 25 \text{ }^\circ\text{C}$  as a function of the integration type of PV system installation (see from [28]).

PV system installation	$c$	$T_M$ ( $G = 1000 \text{ W/m}^2$ , $T_A = 25 \text{ }^\circ\text{C}$ )
Roof-integrated	0.058	83
On top of roof, with small roof-module distance (<10 cm)	0.036	61
On top of roof, with large roof-module distance (>10 cm)	0.027	52
Free-standing	0.02	45

and the average temperature  $T_{\text{avg}}$  of the TE module as

$$T_{\text{avg}} = \frac{1}{2}(T_M + T_A) = T_A + \frac{1}{2}cG \quad (8)$$

where we have used Eq. (5). The efficiency  $\eta_{\text{TE}}$  depends on  $Z$  and on operational temperatures  $T_M$  and  $T_A$ , and thus also depends on irradiance  $G$ .

### 3.4. Annual performance

The annual performance of a PV–TE hybrid is now determined using the above equations and data sets of hourly averaged irradiances and daily averaged ambient temperatures. The annual amount of generated energy (in kWh) is calculated by summing the generated power (W) at each single hour. In order to show differences in climate, we have used datasets for the city of Utrecht, the Netherlands ( $52^\circ 05' \text{N}$ ,  $5^\circ 08' \text{E}$ ), and the city of Malaga, Spain ( $36^\circ 43' \text{N}$ ,  $4^\circ 25' \text{E}$ ). The latter city has higher temperatures and irradiances. Data are taken from the NASA SSE dataset [29], using the simulation tool HOMER [30]. Note that only average daily temperatures were available. The annual distributions of irradiance and temperature are shown in Fig. 2.

## 4. Results

### 4.1. PV efficiency

The efficiency of the PV module as a function of irradiance is shown in Fig. 3, for various temperatures. The STC condition  $T_M = 25 \text{ }^\circ\text{C}$  is shown in the top curve, and the efficiency of the PV module at  $1000 \text{ W/m}^2$  is 14.03%. For different ways of module integration, as indicated in Table 1, different module temperatures result for the same irradiance values, which in turn results in lower efficiency values. Consequently, the higher the coefficient  $c$ , the lower the efficiency. For example, at  $1000 \text{ W/m}^2$  the efficiency of the PV module is 10.78%, as the module temperature is  $83 \text{ }^\circ\text{C}$  for  $c = 0.058$  (roof integrated PV module). Note that for these calculations a constant ambient temperature of  $25 \text{ }^\circ\text{C}$  is used.

### 4.2. TE efficiency

The efficiency of the TE module as a function of irradiance is also shown in Fig. 3, now for a specific figure of merit of  $Z = 0.004 \text{ K}^{-1}$ , which is state-of-the-art for  $\text{Bi}_2\text{Te}_3$  alloys [31]. Depending on the type of integration, the module temperature varies, which is reflected in the four TE efficiency curves. Consequently, the higher the coefficient  $c$ , the higher TE module efficiency becomes. For example, at  $1000 \text{ W/m}^2$  the efficiency of the TE module is 3.20% for  $c = 0.058$ .

The effect of various values for the figure of merit is shown in Fig. 4. The larger  $Z$ , the higher the efficiency, which can amount to 6% or larger for module temperatures above  $80 \text{ }^\circ\text{C}$ .

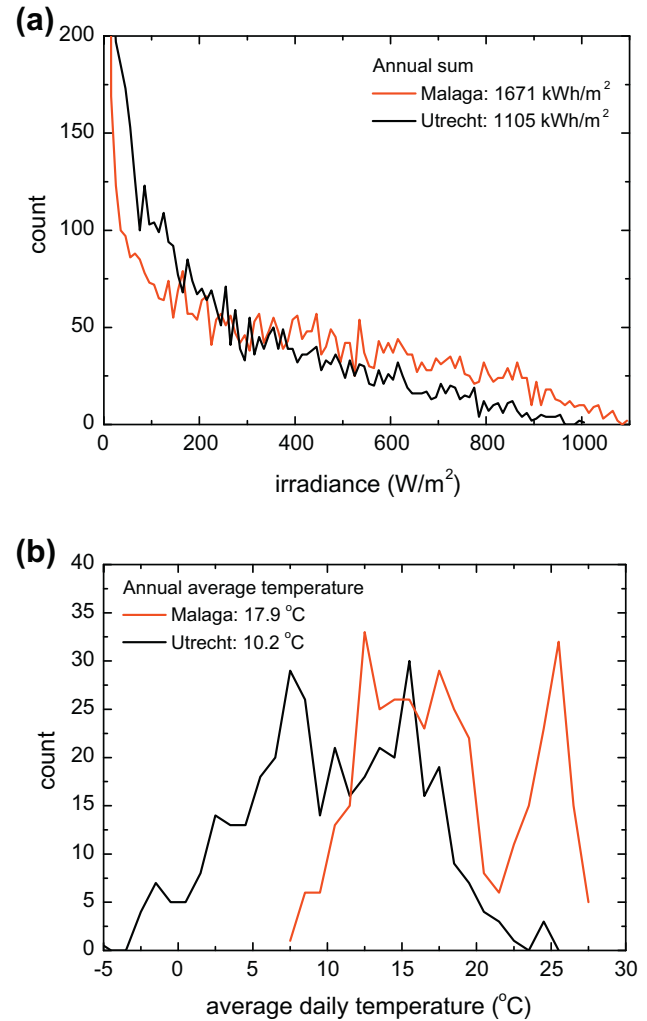


**Fig. 2.** Frequency distribution of irradiance (a) and temperature (b) for the two locations Malaga and Utrecht.

### 4.3. PV–TE generated power

The efficiency of the PV–TE hybrid can now be calculated using Eq. (2), i.e., combining the above results. The generated PV and TE power is depicted in Fig. 5 as a function of irradiance, for the four integration types. Coincidentally, as we will show below, the sum of PV and TE generated power curves closely resembles the generated power as if the PV module would be at constant temperature of  $25 \text{ }^\circ\text{C}$  (STC).

### 4.4. Annual performance

As the irradiance and temperature distributions for Malaga shows higher values than the ones for Utrecht, deploying PV–TE hybrids is expected to lead to a larger efficiency increase in Malaga compared to Utrecht. Fig. 6 shows the generated energy for 10 days in August (19–28) for the city of Malaga. The variation in irradiance is clearly reflected in PV generated energy and TE generated energy. The maximum relative contribution of TE generated energy to the total in this period of 10 days is 24.7% on August 21, the lowest maximum is 11.9% on August 25. A similar graph (not shown) for Utrecht reveals maximum relative contributions of 15.7% and 4.5% on August 21 and 25, respectively.

The PV module deployed in Malaga would yield an annual amount of energy of 211.9 kWh. The TE converter would add an

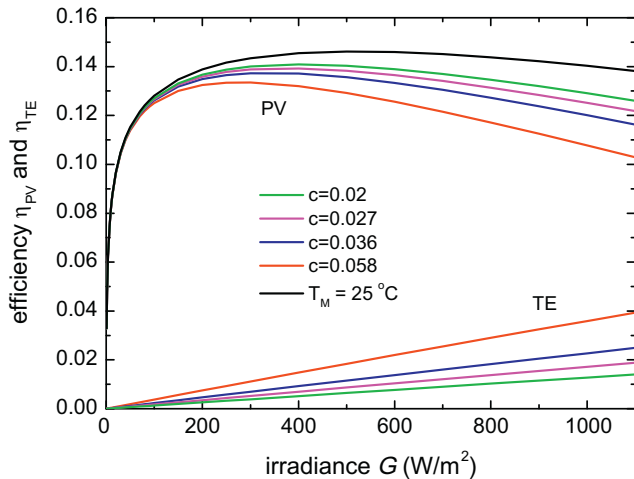


**Fig. 3.** Efficiency of the PV module (marked 'PV') as a function of irradiance for various conditions that result in different module temperatures: STC condition ( $T_M = 25\text{ °C}$ ), and four different ways of module integration as represented by coefficient  $c$  (Eq. (5) and Table 1). Efficiency of the TE module (marked 'TE') for the same four different ways of module integration.

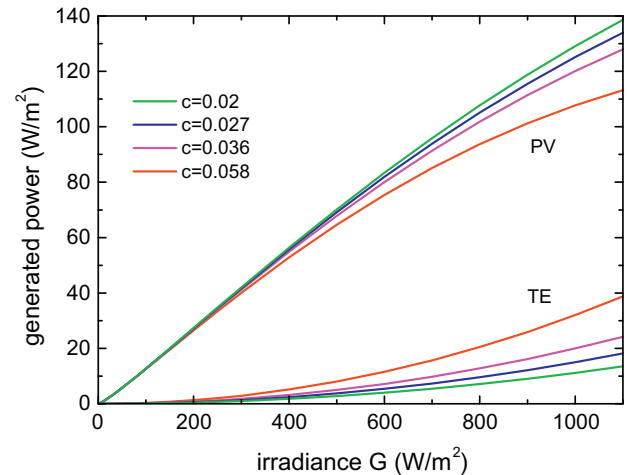


**Fig. 5.** Generated PV and TE power as a function of irradiance for four different ways of module integration.

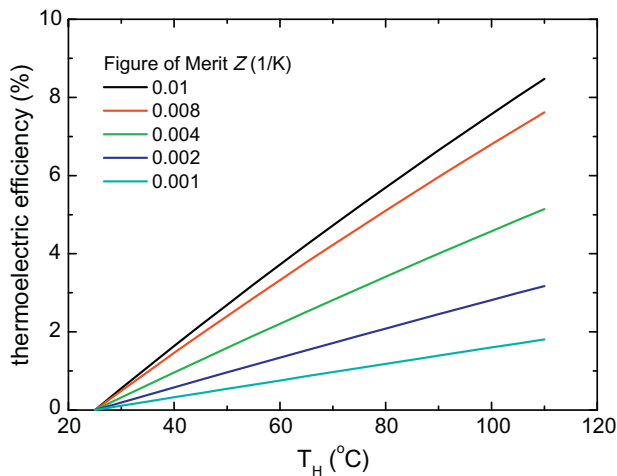


**Fig. 4.** Variation of the thermoelectric efficiency as a function of temperature  $T_H$  for five values of the figure of merit  $Z$ . Note that  $T_L = 25\text{ °C}$ .

additional 31.1 kW h thus totalling 243.0 kW h. The generated energy by the TE converter thus enhances the PV annual energy yield by 14.7%. In case of Utrecht, the PV module would yield 147.4 kW h. Adding 16.1 kW h from the TE converter thus totals 163.6 kW h for the PV–TE hybrid, and the TE converter increases the PV annual energy yield by 11.0%. The higher PV yield for Malaga compared to Utrecht is related to higher irradiances at first order, as for higher irradiances also ambient temperatures are high. The energy generated by the TE converter in Malaga is about twice the amount of that in Utrecht. Note that the average ambient temperature in Malaga is substantially larger than in Utrecht.

## 5. Future developments

Present maximum figure of merit values are  $ZT = 2.5$  as reported for a temperature of 300 K [21], or  $Z = 0.00833\text{ K}^{-1}$ , while  $Z = 0.01\text{ K}^{-1}$  is seen as realistically attainable. However, much more research is needed to explore and explain the observed increases in figure of merit values, especially for new nanomaterial classes such as superlattices and nanowires. Here, one also needs to take into

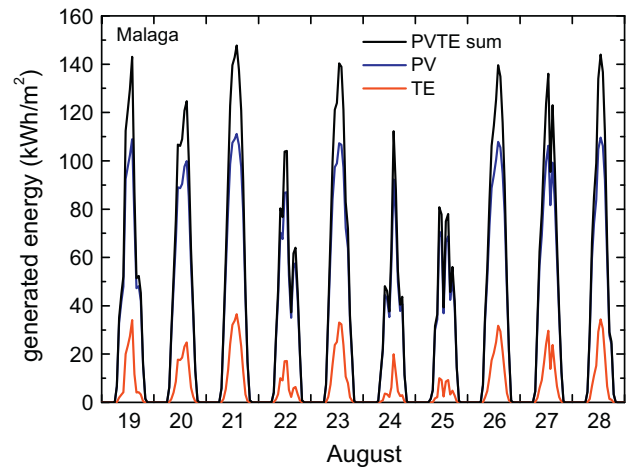


**Fig. 6.** Generated PV, TE, and total energy for a 10-day period in August for the city of Malaga, Spain.

account the possible application area in relation to, e.g., the thickness and heat capacity of such structures. If we assume that a future TE material would have a figure of merit of  $Z = 0.01\text{ K}^{-1}$  at 300 K, thermoelectric efficiencies may be doubled, as can also be seen in Fig. 4. If this material is deployed in a PV–TE hybrid, the irradiance-dependent efficiency as shown in Fig. 7 would be attainable, i.e., for roof-integrated modules ( $c = 0.058$ ). With respect to a PV module efficiency at  $1000\text{ W/m}^2$  of 10.78% (at module temperatures of  $83\text{ °C}$ ), the PV–TE hybrid with  $Z = 0.01\text{ K}^{-1}$  shows an efficiency of 16.11%, or 50% larger than for a PV module alone. For the present near-maximum value of  $Z = 0.008\text{ K}^{-1}$  an PV–TE efficiency of 15.56% is reached, while for  $Z = 0.002\text{ K}^{-1}$  (reported for silicon nanowires [24]) an efficiency of 12.73% can be reached. For comparison, also the efficiency of a PV module is shown, for a constant module temperature of  $25\text{ °C}$  (STC). The PV–TE efficiency curve for  $Z = 0.004\text{ K}^{-1}$  (present today's maximum) coincidentally coincides with the STC curve.

The annual performance of the future PV–TE hybrid deployed in Malaga with  $Z = 0.01\text{ K}^{-1}$  would be enhanced to 264.6 kW h, which is 8.9% larger than for the PV–TE hybrid with  $Z = 0.004\text{ K}^{-1}$ . In case of Utrecht, the annual performance would be enhanced to 174.8 kW h, or a 6.7% larger than the  $Z = 0.004\text{ K}^{-1}$  PV–TE hybrid. Compared to a PV module alone a performance enhancement of 24.9% and 18.6% is calculated, for Malaga and Utrecht, respectively.



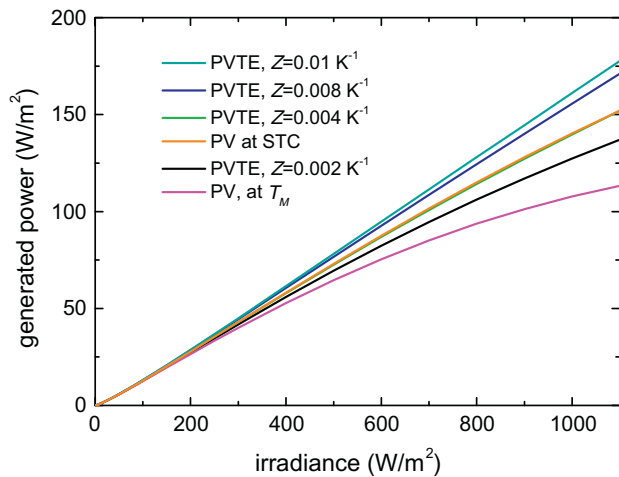


Fig. 7. Generated PVTE power as a function of irradiance for four values of the figure of merit  $Z$ , and generated PV power as a function of irradiance at STC and actual module temperature  $T_M$  determined by irradiance level.

## 6. Discussion

### 6.1. Loss

The model described above allows for a calculation of the maximum enhancement of efficiency as a result of adding a TE converter. Several losses are not considered, such as reflection losses, which typically amount to 5–10% for PV modules. Heat flux and radiation losses from the side and front cover are also not taken into account. Further, although it is yet unclear if such arrangement may be realized in practice, it is assumed that the back side temperature of the TE converter always equals the ambient temperature. This is a critical assumption, and may not be realized in practice. Clearly, a higher back side temperature lowers the TE efficiency and possible benefits are thus reduced. As an example, if the temperature difference between front and back side would be lowered to 75% of its value (by enhancing the back side temperature), the TE efficiency at  $1000 \text{ W/m}^2$  and  $T_M = 83 \text{ }^\circ\text{C}$  would be lowered from 3.59% to 2.68% (or nearly 25% lower). While the TE efficiency is substantially lowered, the annual energy yield is affected to a much lesser extent, which is of course due to the relatively low (around 10%) contribution of TE generated energy to the total amount. The annual energy yield in case of Malaga is found to be lowered from 243.0 kWh to 235.2 kWh, or only 3.3% lower, while the contribution from the TE converter is reduced from 31.1 kWh to 23.3 kWh (25% reduction). For Utrecht, the annual energy yield is lowered from 163.6 kWh to 159.4 (2.6% lower). From the above we therefore estimate that the PV–TE efficiencies calculated by the simple and idealized model may in practice be substantially lower, but as the contribution of the TE converter to the total is relatively small, the generated power may be lower by about 10% only.

### 6.2. Cost

Besides the theoretical benefits a TE module can have on the performance of a PV module, the extra cost of applying the TE module is important: it should be balanced by the extra power output due to the TE module.

Commercial TE modules for cooling are available in many sizes, from microsize to cm-size. For example, one company offers a range of modules from  $2.2 \times 4.2 \text{ mm}^2$  to  $62 \times 62 \text{ mm}^2$  size, ranging in power from 0.5 to 200 W [32]. Prices (10–24 pieces) range from  $\sim 0.1 \text{ } \$/\text{W}$  (large size) to  $\sim 50 \text{ } \$/\text{W}$  (small size). Note that typically

for large quantities prices may easily be halved. The  $62 \times 62 \text{ mm}^2$  sized module has a cooling capacity of 270–400 W, depending on operating voltage and thickness; cooling capacity ranges from 0.05 to  $0.1 \text{ W/cm}^2$ .

TE modules for generating electricity are found in the same sizes as the cooling ones. Typical numbers are 5–10  $\text{\$/W}$  for  $50 \times 50 \text{ mm}^2$  modules of  $0.3\text{--}0.5 \text{ W/cm}^2$ . Extra cost for a PV–TE hybrid should be not more than about 10% of the  $\text{m}^2$  price of a module, which is presently at about 3  $\text{\$/W}$ , hence  $450 \text{ } \$/\text{m}^2$ , for a 15% efficiency PV module. If adding TE converters that lead to 10% increase in power, thus a  $165 \text{ W/m}^2$  PV–TE hybrid, extra cost allowed is only 45\$. Applying TE modules over the whole backside of the PV module is not needed, as the cooling capacity in  $\text{W/cm}^2$  is 3–5 times larger than incident solar power. Nevertheless, extra cost would be about one order of magnitude larger than the PV module cost alone, which is unacceptable, and may limit widespread use of thermoelectrics [33].

In summary, the required increase in efficiency as outlined above, another very important issue is to reduce the cost, by at least one order of magnitude. As new, high efficient TE modules are still being developed, present high prices should come down with increased amounts of units produced, following experience curve theory, see, e.g., [34].

## 7. Conclusions

We have developed a simple model to determine the efficiency of a combined photovoltaic and thermoelectric converter, or PV–TE hybrid. The model is applied to certain types of integrated PV–TE hybrids. Results show that adding a TE converter to the backside of a PV module can lead to an efficiency increase of 8–23%, depending on the type of module integration, and assuming TE material with a typical present day figure of merit value of  $Z = 0.004 \text{ K}^{-1}$ . The efficiency increase critically depends on the assumption that the backside is sufficiently cooled such that it is at ambient temperature. The annual performance of a PV–TE hybrid is modelled using two annual irradiance and temperature profiles, i.e., for Malaga, Spain, and Utrecht, the Netherlands, and is found to increase by 14.7% and 11%, for Malaga and Utrecht, respectively.

Future developments in TE material research may allow for figure of merit values of  $Z$  that approach  $Z = 0.01 \text{ K}^{-1}$ . These high- $Z$  materials would allow for an efficiency increase of up to 50%. The effect on annual performance is lower, but varies between 24.9% and 18.6% for the two cases studied.

The efficiency and performance enhancements are calculated using a simple, idealized model. Practical TE efficiencies are estimated to be 25% lower, while performance is less affected and are estimated to be about 10% lower. Present cost prohibit the use of TE in PV–TE hybrids. It is imperative that the calculated performance of a PV–TE hybrid is validated by appropriate experiments; these will be performed in our outdoor PV test set-up.

## Acknowledgements

We gratefully acknowledge Dejan Gajic, Jeroen Rodenburg, and Matthijs Vakar (Junior College Utrecht, the Netherlands) for enthusiastic exploratory work, and Nils Reich for critical reading of the manuscript. SenterNovem is acknowledged for financial support as part of the Dutch Nieuw Energie Onderzoek (New Energy Research) programme.

## References

- [1] Drews A, de Keizer AC, Beyer HG, Lorenz E, Betcke J, van Sark WJGHM, et al. Monitoring and remote failure detection of grid-connected PV systems based on satellite observations. *Solar Energy* 2007;81:548–64.

- [2] Royne A, Dey CJ, Mills DR. Cooling of photovoltaic cells under concentrated illumination: a critical review. *Solar Energy Mater Sol Cells* 2005;86:451–83.
- [3] Chou SK, Yang WM, Chua KJ, Li J, Zhang KL. Development of micro power generators – A review. *Appl Energy* 2011;88:1–16.
- [4] Zondag HA. Flat-plate PV-Thermal collectors and systems: a review. *Renew Sustain Energy Rev* 2008;12:891–959.
- [5] Chow TT. A review on photovoltaic/thermal hybrid solar technology. *Appl Energy* 2010;87:365–79.
- [6] Ellion EM. Combined photovoltaic-thermoelectric solar cell and solar cell array. Patent WO 88/02556; 1988.
- [7] Rockendorf G, Sillmann R, Podlowski L, Litzenburger B. PV-hybrid and thermoelectric collectors. *Solar Energy* 1999;67:227–37.
- [8] Vorobiev Y, González-Hernández J, Vorobiev P, Bulat L. Thermal-photovoltaic solar hybrid system for efficient solar energy conversion. *Solar Energy* 2006;80:170–6.
- [9] Tritt TM, Böttner H, Chen L. Thermoelectrics: direct solar thermal energy conversion. *MRS Bull* 2008;33:366–8.
- [10] Muhtaroglu A, Yokochi A, Von Jouanne A. Integration of thermoelectrics and photovoltaics as auxiliary power sources in mobile computing applications. *J Power Sources* 2008;177:239–46.
- [11] Imenes AG, Mills DR. Spectral beam splitting technology for increased conversion efficiency in solar concentrating systems: a review. *Solar Energy Mater Solar Cells* 2004;84:19–69.
- [12] Riffat SB, Ma X. Thermoelectrics: a review of present and potential applications. *Appl Therm Eng* 2003;23:913–35.
- [13] Xi H, Luo L, Fraisse G. Development and applications of solar-based thermoelectric technologies. *Renew Sustain Energy Rev* 2007;11:923–36.
- [14] Rowe DM, editor. CRC handbook of thermoelectrics. London, NY, USA: CRC Press; 1995.
- [15] Ioffe AF. Semiconductor thermoelements and thermoelectric cooling. London, UK: Infosearch Ltd.; 1957.
- [16] Omer SA, Infield DG. Design optimization of thermoelectric devices for solar power generation. *Solar Energy Mater Solar Cells* 1998;53:67–82.
- [17] Poudel B, Hao Q, Ma Y, Lan Y, Minnich A, Yu B, et al. High-thermoelectric performance of nanostructured bismuth antimony telluride bulk alloys. *Science* 2008;329:634–8.
- [18] Zhang T, Zhang Q, Jiang J, Xiong Z, Chen J, Zhang Y, et al. Enhanced thermoelectric performance in p-type BiSbTe bulk alloy with nano-inclusion of ZnAlO. *Appl Phys Lett* 2011;98:022104.
- [19] Dresselhaus MS, Chen G, Tang MY, Yang R, Lee H, Wang D, et al. New directions for low-dimensional thermoelectric materials. *Adv Mater* 2007;19:1043–53.
- [20] Kanatzidis MG. Nanostructured thermoelectrics: the New Paradigm? *ChemMater* 2010;22:648–59.
- [21] Böttner H, Chen G, Venkatasubramanian R. Aspects of thin-film superlattice thermoelectric materials, devices, and applications. *MRS Bull* 2006;31:211–7.
- [22] Kovalenko MV, Spokoyny B, Lee J-S, Scheele M, Weber A, Perera S, et al. Semiconductor nanocrystals functionalized with antimony telluride Zintl ions for nanostructured thermoelectrics. *J Am Chem Soc* 2010;132:6686–95.
- [23] See KC, Feser JP, Chen CE, Majumdar A, Urban JE, Segalman RA. Water-processable polymer-nanocrystal hybrids for thermoelectrics. *Nano Lett* 2010;10:4664–7.
- [24] Hochbaum AI, Chen R, Delgado RD, Liang W, Garnett EC, Najarian M, et al. Enhanced thermoelectric performance of rough silicon nanowires. *Nature* 2008;451:163–7.
- [25] Boukai AI, Bunimovich Y, Tahir-Kheli J, Yu JK, Goddard III WA, Heath JR. Silicon nanowires as efficient thermoelectric materials. *Nature* 2008;451:168–71.
- [26] Vining CB. Desperately seeking silicon. *Nature* 2008;451:132–3.
- [27] Reich NH, Van Sark WGJHM, Alsema EA, Lof RW, Schropp REI, Sinke WC, et al. Crystalline silicon cell performance at low light intensities. *Solar Energy Mater Solar Cells* 2009;93:1471–81.
- [28] Sauer DU. Untersuchungen zum Einsatz und Entwicklung von Simulationsmodellen für die Auslegung von Photovoltaik-Systemen. Thesis. TH Darmstadt; 1994.
- [29] NASA Atmospheric Sciences Data Center. Surface meteorology and Solar Energy (web site). <<http://eosweb.larc.nasa.gov/sse>> [accessed February 2011].
- [30] Lambert T, Gilman P, Lienthal P. Micropower system modeling with HOMER. In: Farret FA, Simões MG, editors. Integration of alternative sources of energy. New York, USA: Wiley; 2006. p. 379–418.
- [31] Yamashita O, Tomiyoshi S, Makita K. Bismuth telluride compound with high thermoelectric figures of merit. *J Appl Phys* 2003;93:368–74.
- [32] Custom Thermoelectrics. <<http://www.customthermoelectric.com/>>.
- [33] Vining CB. An inconvenient truth about thermoelectrics. *Nat Mater* 2009;8:83–5.
- [34] Van Sark WGJHM, Alsema EA, Junginger HM, De Moor HHC, Schaeffer GJ. Accuracy of progress ratios determined from experience curves: the case of photovoltaic technology development. *Prog Photovolt Res Appl* 2008;16:441–53.